A Novel Full-Angle Detection Method for Bolt Loosening Based on Color Segmentation

Jingjie Kang, Lijun Zhang*, Yuandong Sun, Xiaoyu Yang, Ruolan Wang and Tianhao Zhao

{*Corresponding author kangjingjie24@193.com}
{ kangjingjie23@163.com, sunyd2006lzu@163.com, yangxiaoyu@163.com, wangruolan@163.com, zhaotianhao@163.com}

Mechanical Properties Group, Physical Testing & Chemical Analysis Center of Metallic Materials of China Ordnance Industry, Ningbo, China

Abstract: In response to the existing problem of the inability to perform full-angle detection of bolt loosening based on anti-loosening lines segmentation, this paper develops a method based on color segmentation and directional vector calculation. Initially, the anti-loosening line image is segmented using an optimal threshold segmentation method for the R component and a non-linear stretching method for the a component under the transformation of Lab and RGB color spaces. Subsequently, morphological operations are performed on the image using an open operation. Then, the minimum bounding rectangle of the anti-loosening line connected domain area is determined through an angle progressive minimum encapsulation method, and its directional vector is established. Consequently, the full-angle of bolt loosening is calculated based on the four-quadrant arctangent function and specific adjustments. Finally, an experimental scheme is designed to validate the feasibility and accuracy of the proposed algorithm. The experimental results show that the detection algorithm can achieve a 0 to 360-degree loosening angle detection of bolts, with a maximum absolute error of 0.6345 degrees and a maximum relative error of 0.75%. The accuracy of the algorithm can meet the needs of engineering practice and exhibits significant potential for application.

Keywords: Bolt Looseness Detection, Full-angle Detection, Color Segmentation, Nonlinear Stretching, Vector Calculation

1. Introduction

As a typical fastener in modern industrial standards, bolts play a crucial role in various fields such as aviation[1], aerospace[2], marine vessels[3], and land-based tanks[4]. However, due to mechanical vibrations during the operation of fastened structural components or inherent defects in casting materials, failures such as loosening and fatigue fractures in bolts can occur, resulting in incalculable losses[5]. To ensure the safe and effective service of bolts, regular inspection and fastening are of paramount importance[6]. Compared to traditional manual or contact-based inspection and

ICSETPSD 2023, November 17-18, Coimbatore, India

DOI 10.4108/eai.17-11-2023.2342751

maintenance methods, utilizing image processing and analysis methods in machine vision-based automatic bolt inspection equipment offers advantages such as non-contact operation, traceability, and high levels of intelligent development[7].

The existing research on visual detection methods for bolt loosening primarily consists of two approaches: traditional image processing and deep learning. In traditional image processing, the mainstream methods involve first using Hough circle detection methods[8]-[10] to locate the bolts. Then, algorithms such as Hough transform[11] and RAMMER[12] are used to detect the variation in slope of the edge lines before and after bolt loosening, enabling the calculation of the loosening angle. On the other hand, deep learning methods mainly utilize a series of deep learning algorithms to detect the bolt region[13]-[15]. Subsequently, techniques such as optical flow-based object detection methods[16], target-based methods[17]、[18], and feature matching methods[19] are employed to detect the differences before and after bolt loosening, allowing for the quantification of the loosening angle. Despite their broad applicability to bolt scenarios, current deep learning-based methods face challenges in achieving universal localization using a single recognition model. Traditional image processing methods, on the other hand, often encounter unavoidable false detections due to complex scenes and uneven lighting in bolt service environments.

Inspired by the existing manual visual inspection method, which involves marking anti-loosening lines on bolts for rapid initial assessment of their service status, many researchers have utilized the noticeable color difference between the anti-loosening lines and the surrounding environment to locate the bolt area. Furthermore, they have conducted corresponding studies on the shape characteristic variations of the anti-loosening lines before and after bolt loosening to qualitatively characterize the behavior of bolt loosening[20]-[23]. By transforming the complex task of recognizing the overall shape characteristics of bolts into a single line recognition problem, our approach offers significant advantages in terms of computational cost and universality compared to the two aforementioned methods. While previous research has provided valuable insights into bolt loosening, there has been a lack of quantitative studies specifically focusing on the detection of bolt loosening angles, particularly across the comprehensive range of 0 to 360 degrees. Full-angle detection, as opposed to angle-limited detection, plays a crucial role in establishing the relationship between bolt loosening angles and preload force loss[24], as well as in various studies such as the improvement of automatic inspection devices for unmanned aerial vehicles and the quantitative tightening of bolts[25].

In response to the aforementioned issues, this paper presents a novel method for the full-angle detection of bolt loosening based on anti-loosening lines segmentation. Firstly, a color segmentation method is designed using the Lab and RGB color spaces, which involves non-linear stretching of the a-component and optimal threshold segmentation of the R-component to extract the red anti-loosening lines region. Next, an opening operation is applied to optimize the segmentation results by refining the segmented region. Subsequently, the minimum bounding rectangle of the anti-loosening line is determined, and the direction vector of the line is computed. Then, the angular deviation between the two direction vectors of the anti-loosening lines is calculated. Finally, the effectiveness of the proposed method for full-angle detection of bolt loosening is validated through experimental evaluation.

2. Method

The research scenario of this study is illustrated in Figure 1. Anti-loosening lines are marked on the bolt and the base, and the angle formed by these lines is used to quantify the degree of bolt loosening. The anti-loosening line that rotates along with the bolt as it loosens is referred to as the rotating anti-loosening line, while the anti-loosening line that serves as a reference on the base is called the fixed anti-loosening line.Based on this research scenario, the overview of the proposed method is presented in Figure 2.

Fig.1 Research scenario.

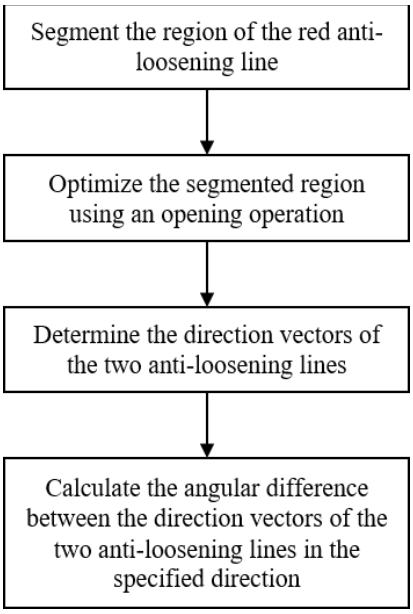

Fig.2 Overview of the method.

First, a color segmentation method is employed to segment the red anti-loosening line region. This method involves non-linear stretching of the a component in the Lab color space and optimal thresholding of the R component in the RGB color space. By applying this approach, the red anti-loosening line region can be effectively separated from the background.

Next, we perform an opening operation on the segmented anti-loosening line image to remove unnecessary connected regions while preserving the integrity of the anti-loosening line image.

Afterward, the minimum bounding rectangles of the two anti-loosening lines are identified, and the direction vectors of the lines are determined.

Subsequently, the angle-progression minimum enclosing rectangle method is employed to individually identify the minimum bounding rectangles for both anti-loosening lines and determine their direction vectors.

Finally, the four-quadrant tangent and cotangent functions, along with an angle rule, are utilized to calculate the angle between the direction vectors of the two anti-loosening lines in the specified direction.

3. Principle of Method

3.1 Anti-Loosening Lines Segmentation based on Color Space Conversiona)

a) Color Space Conversion: In image processing, various color spaces such as RGB, HSV, and Lab are commonly used to describe images. Among them, RGB color space is the most widely used . The RGB color space divides the image into three

components: R (red), G (green), and B (blue), and by combining these three components, it can represent a wide range of colors in the real world. It is commonly used in image display on monitors. However, when it comes to the segmentation of red-colored markers like anti-loosening lines, the Lab color space has the advantage of higher component separability and is less affected by illumination. It is also more perceptually uniform, making it more efficient for the segmentation of red pixels. The Lab color space consists of the L (lightness) component and the a and b color-opponent components. Since Lab and RGB color spaces cannot be directly converted, a two-step process is used: first, the RGB color space is converted to the XYZ intermediate color space, and then it is further converted to the Lab color space model[26].

RGB color space to XYZ color space conversion, the conversion process is as follows:

$$\begin{bmatrix} X \\ Y \\ Z \end{bmatrix} = \boldsymbol{M} \times \begin{bmatrix} R \\ G \\ B \end{bmatrix}, \boldsymbol{M} = \begin{bmatrix} 0.4124 & 0.3567 & 0.1805 \\ 0.2126 & 0.7152 & 0.0722 \\ 0.0193 & 0.1192 & 0.9505 \end{bmatrix} \tag{1}$$

Then, XYZ color space to Lab color space conversion, the conversion process is as follows:

$$\begin{cases} L = 116 f\left(\dfrac{Y}{Y_n}\right) - 16 \\ a = 500\left[f\left(\dfrac{X}{X_n}\right) - f\left(\dfrac{Z}{Z_n}\right) \right] \\ b = 200\left[f\left(\dfrac{X}{X_n}\right) - f\left(\dfrac{Z}{Z_n}\right) \right] \end{cases} \tag{2}$$

$$f(t) = \begin{cases} t^{\frac{1}{3}} & \text{if } t > \left(\dfrac{6}{29}\right)^3 \\ \dfrac{1}{3}\left(\dfrac{29}{6}\right)^2 t + \dfrac{4}{29} & \text{otherwise} \end{cases}$$

Where X_n, Y_n, and Z_n are the stimulus values of the primary colors XYZ under white light conditions, with values as follows:

$$\begin{cases} X_n = 96.4221 \\ Y_n = 100 \\ Z_n = 82.5221 \end{cases} \tag{3}$$

To eliminate the influence of illumination in subsequent image segmentation, the high component separability of the Lab color space can be utilized. By removing the

L (brightness) and b components from the Lab color space model (setting them to 0), only the a component is considered for analysis. As shown in Figure 3, after processing the original image (left image in Figure 3) and converting it to the RGB color space from the Lab color space, the segmented image of the anti-loosening line (right image in Figure 3) is obtained. However, there are several noise points in the surrounding area.

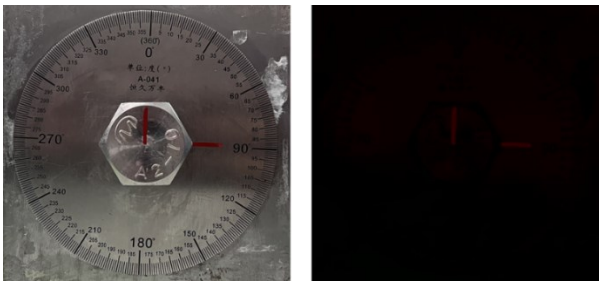

Fig.3 Illustration of the RGB color space after processing with consideration only for the a component following Lab color space conversion.

b) Nonlinear Stretching of the a Component: In the Lab color space, the positive axis of the a component represents the degree to which a pixel is close to the color red. In order to highlight the significant difference between red pixels and the background in a more intuitive way and make the algorithm more efficient, a nonlinear function is applied to stretch the a component. The goal of stretching is to enhance the red pixels while minimizing the impact on the colors of other pixels. The stretched a component is given by Equation (4).

$$\boldsymbol{a}_{\text{new}}\left(\text{i},\text{j}\right)=k_1*\boldsymbol{a}\left(\text{i},\text{j}\right)^{k_2} \tag{4}$$

In the equation, $\boldsymbol{a}\left(\text{i},\text{j}\right)$ represents the value of the a component of the pixel $\left(\text{i},\text{j}\right)$ in the original image, and $\boldsymbol{a}_{\text{new}}\left(\text{i},\text{j}\right)$ represents the value of the a component of the pixel $\left(\text{i},\text{j}\right)$ in the stretched image. The parameters k_1 and k_2 are used in the non-linear transformation. For this particular case, suitable parameter values are chosen as $k_1=0.5$ and $k_2=2$. The stretching effect is illustrated in Figure 4, where the stretched image's a component is converted to the RGB color space (shown on the right), and it exhibits a more vibrant red color for the marked line compared to the original RGB color space (shown on the left). Combining the findings from Section *A*, the effect of considering only the a component is shown in Figure 5.

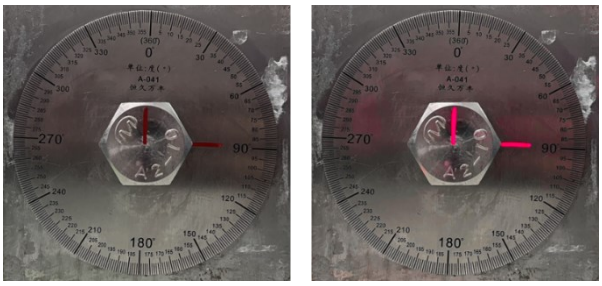

Fig.4 Comparison of a Component Before and After Non-linear Stretching

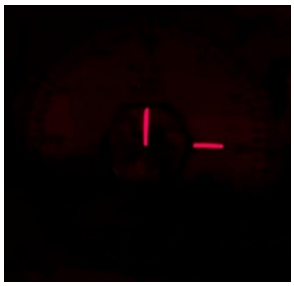

Fig.5 Illustration of Processing Only the a Component

c) Segmentation of Marker Lines in the Original Image: By combining Sections b and c, the marker lines in the original image were considered by focusing solely on the a component and applying non-linear stretching. After converting the image to the RGB color space, the marker lines became more prominent and easier to segment. The stretched a component in the Lab space, when transformed to the RGB color space, is shown in Figure 6 (right).

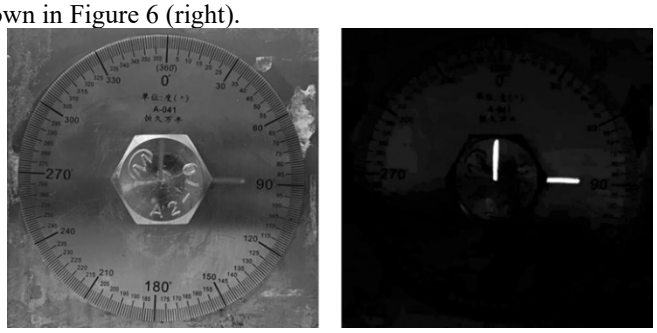

Fig.6 Left: Original image; Right: R component after non-linear stretching of the a component and conversion to the RGB color space

Compared to the left image in Figure 6, the right image shows only the red anti-loosening line image and noticeable noise points that are introduced by the non-linear stretching of the a component. To address this, the OTSU algorithm[27] is considered for segmentation of the R component of the image. The segmentation results are shown in Figure 7.

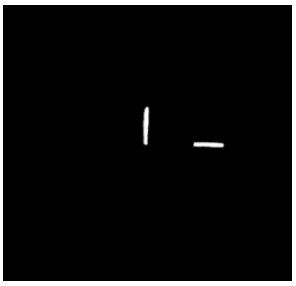

Fig.7 Segmentation Result of the Anti-loosening Line Image

3.2 Morphological image processing

After the segmentation of the image based on color space, there are usually connected regions in the image that are not part of the target bolt region. To facilitate the subsequent algorithms, morphological operations are used to eliminate these non-target regions. The opening operation from morphological operations is employed for this purpose, following the equation (5). The opening operation involves the erosion of the connected region set A in the image using a structuring element B, followed by the dilation of the eroded result using B[28].

$$A \circ B = \left(A \odot B \right) \oplus B \tag{5}$$

Here, $\odot$ represents the erosion operation in morphological processing, and $\oplus$ represents the dilation operation in morphological processing.

3.3 Minimum Enclosing Rectangle of the Smallest Area for Anti-Loosening Line Connected Components

After applying morphological operations to the image from Figure 7, we assign the connected component of the rotating anti-loosening line as "markLine1" and the connected component of the fixed anti-loosening line as "markLine2". To determine the orientation vectors of the two anti-loosening lines, we propose a method based on the progressive minimum bounding rectangle algorithm to find the minimum enclosing rectangle that reflects the direction of the connected component. Taking "markLine2" as an example, the procedure for determining the minimum enclosing rectangle of the connected component's area is as follows:

Step 1: Start by drawing a bounding rectangle that is parallel to the image's horizontal and vertical axes, with one side equal to the longer side of the connected component and the other side equal to the shorter side. Record the area S of this rectangle.

Step 2: Rotate the target image counterclockwise around a fixed point on the image. For any point $\left(x_{i1}, y_{i1}\right)$ on the target image, its corresponding point $\left(x_{i2}, y_{i2}\right)$ after rotation by an angle α around the fixed point $\left(x_0, y_0\right)$ can be calculated using the following equation (6):

$$\begin{cases} x_{i2} = (x_{i1} - x_0)\cos(\alpha) - (y_{i1} - y_0)\sin(\alpha) + x_0 \\ y_{i2} = (x_{i1} - x_0)\sin(\alpha) - (y_{i1} - y_0)\cos(\alpha) + y_0 \end{cases} \quad (6)$$

Step3. Rotate the target image from 0 to 90 degrees with an interval of 1 degree. For each rotation, calculate the area, vertices, and rotation angle of the minimum bounding rectangle of the rotated image.

Step4. Compare the areas of the bounding rectangles obtained during the rotation process and record the rectangle with the smallest area. Take note of its vertex coordinates and rotation angle.

Step5. Rotate the rectangle obtained in Step 4 in the opposite direction by the same angle to obtain the minimum bounding rectangle.

The minimum bounding rectangle of markLine2, obtained using the above method, is shown in Figure 8. The right image is an enlarged illustration. The process of finding the minimum bounding rectangle for markLine1 is similar.

Fig.8 Minimum bounding rectangle of markLine2

3.4 Calculation of the Angle between MarkLine Vectors Based on Vector Processing

In accordance with the definition specified in Section C, the vector along the longer side of the minimum bounding rectangle, originating from the center of the image and extending towards the image boundary, is designated as the direction vector of the anti-loosening line. Please refer to Figure 9 for visual representation.

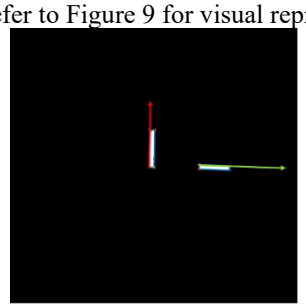

Fig.9 Direction vector of the anti-loosening line

The two direction vectors are normalized, and the unit vector of the rotating anti-loosening line is denoted as e1, while the unit vector of the fixed anti-loosening line is denoted as e2. Refer to equation (7), where the angle formed between a vector and the x-axis can be calculated using the atan2 (four-quadrant arctangent) function, which provides a range of (-π, π]. If the resulting angle from the function is positive, then the angle value is within the range of (0, π], representing the counterclockwise direction. If the resulting angle is negative, then the angle value is within the range of (-π, 0], representing the clockwise direction[29].

$$\theta_1 = \text{atan2}(\boldsymbol{e}_1), \theta_2 = \text{atan2}(\boldsymbol{e}_2) \tag{7}$$

Since bolt loosening occurs in a single direction, we can define counterclockwise as the direction of bolt loosening. If the clockwise direction is considered as the loosening direction, the research process remains the same. As counterclockwise bolt loosening covers a total angle of 360°, the adjustment is made as shown in equation (8).

$$\theta = \begin{cases} |\theta_1 - \theta_2| & \text{if } \theta_1 < 0 \text{ and } \theta_2 \geq 0 \\ |\theta_1 + \theta_2| & \text{if } \theta_1 < 0 \text{ and } \theta_2 < 0 \\ 360 - \theta_1 + \theta_2 & \text{if } \theta_1 \geq 0 \text{ and } \theta_2 > 0 \\ 360 - \theta_1 - \theta_2 & \text{if } \theta_1 \geq 0 \text{ and } \theta_2 < 0 \end{cases} \tag{8}$$

where θ is the angle between vector $\boldsymbol{e}_2$ and $\boldsymbol{e}_2$.

4. Experimental Results and Analysis

To validate the effectiveness and practicality of the proposed rotation angle detection method, an experimental platform was set up as shown in Figure 10. In the experimental setup, a circular gauge fixed on the surface of a steel plate was used for validating the accuracy of bolt angle detection. An M20 bolt was threaded through the gauge, which can be removed in practical applications. The fixed anti-loosening line markLine2 was drawn on the circular gauge, and the rotating anti-loosening line markLine1 was drawn on the surface of the bolt. Image capture was performed using the built-in camera of an iPhone 13 mini smartphone, with the camera parameters listed in Table 1. The distance between the camera and the experimental setup was 25 cm. The image processing algorithm was implemented on an Intel i7 hardware platform with 32 GB of memory and an NVIDIA Quadro T1000 graphics card. The software environment used was Windows 11 and MATLAB R2019a. The experimental validation results for the detection of bolt loosening over the full angle range are presented in Table 3. The selected parameters for the algorithm are listed in Table 2.

Table 1. Camera Parameters.

Parameters	Value

Aperture	f/1.6
Focal Length	53mm
Resolution	3024×3024

Table 2. Parameters Selected in This STUDY

Parameters	**Parameters**
k_1	0.00005
k_2	5
Shape of Structuring Element B	Square
Size of Structuring Element B	3×3

The experimental results demonstrate that the proposed method is capable of detecting bolt loosening angles in the range of 0 to 360 degrees. The maximum absolute measurement error is 0.6345 degrees, with a maximum relative error of 0.75%. The detection accuracy remains relatively stable for angles at any value and complies with the practical engineering error standards, indicating a high level of measurement precision. Specifically, for loosening angles in the range of 0 to 30 degrees, the absolute error does not exceed 0.23 degrees, and the relative error does not exceed 0.75%. The method also exhibits good performance in monitoring the early-stage relaxation of bolts. The main sources of detection errors are as follows: 1. Marking of the anti-loosening line, as the core of this method relies on the angle formed by the anti-loosening line for quantifying the bolt loosening angle. The direction of the marked anti-loosening line can influence the calculation in Equation (7) and subsequently affect the final detection angle. 2. Segmentation effectiveness of the color segmentation algorithm. Since the color segmentation method used in this study is a global segmentation approach, it may exhibit certain errors in determining the edge colors of the anti-loosening line, thereby affecting the subsequent determination of the minimum bounding rectangle of the connected domain in the algorithm. 3. Measurement errors of the circular gauge for bolt loosening. The actual loosening angle of the bolt, used as a reference for comparison with the detection results, is manually measured using a circular gauge, which introduces a certain degree of measurement error.

5. Conclusion

This study developed a comprehensive bolt loosening detection method based on anti-loosening lines segmentation. The proposed method combines techniques such as color space conversion, image segmentation, and directional vector processing, providing a reliable and efficient solution for bolt loosening assessment. Through theoretical description and experimental validation, a novel quantitative angle detection strategy distinct from existing methods has been achieved. By utilizing the camera of a smartphone as the data acquisition device, quantitative detection of loosely

tightened bolts marked with anti-loosening lines was performed, with a maximum measurement error of 0.6345 degrees and a relative error of 0.75%. These results demonstrate that the method offers the advantages of high precision and low cost while enabling automated and non-contact full-angle measurement of bolt loosening. Future research could explore wider practical applications, considering scenarios such as tilted bolts and expanding the scope of the proposed method.

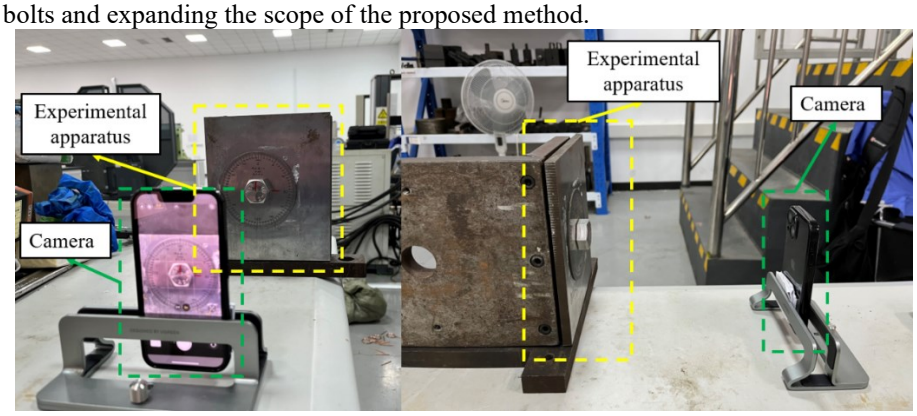

Fig.10 Experimental platform.

Table 3. Measurement Results of Bolt Loosening Full Angle

Actual value (°)	Calculated value (°)	Diference value (°)	Error rate (%)
5	5.036	0.036	0.72
10	10.0718	0.0718	0.72
30	29.7745	0.2255	0.75
60	59.6193	0.3807	0.63
100	100.2092	0.2092	0.21
120	119.6354	0.3646	0.30
150	150.6345	0.6345	0.42
180	179.593	0.407	0.23
240	240.0046	0.0046	0.00
300	300.1514	0.1514	0.05
350	349.9932	0.0068	0.00
360	359.4537	0.5463	0.15

References

[1] Firsov V A, Bekhmet'ev V I. Single-impact calibrated electromagnetic tightening of long-life bolted joints in aviation structures[J]. Ensuring the Reliability and Service Life of Flight Vehicle Structures by Engineering Methods, 1991: 4-8.

[2] Champaney L, Boucard P A, Guinard S. Adaptive multi-analysis strategy for contact problems with friction: Application to aerospace bolted joints[J]. Computational

Mechanics, 2008, 42(2): 305-315.
[3] Gaiotti M, Ravina E, Rizzo C M, et al. Testing and simulation of a bolted and bonded joint between steel deck and composite side shell plating of a naval vessel[J]. Engineering Structures, 2018, 172: 228-238.
[4] Malhotra P. Practical nonlinear seismic analysis of tanks[J]. Earthquake spectra, 2000, 16(2): 473-492.
[5] Gong H, Ding X, Liu J, et al. Review of research on loosening of threaded fasteners[J]. Friction, 2022, 10(3): 335-359.
[6] Heselmans J, Vermeij P. Fatal accident in Dutch swimming pool caused by environmentally cracked bolts[C]//CORROSION 2013. OnePetro, 2013.
[7] Ye X W, Dong C Z, Liu T. A review of machine vision-based structural health monitoring: methodologies and applications[J]. Journal of Sensors, 2016, 2016.
[8] Park J H, Kim T H K, Lee K S, et al.Novel bolt-loosening detection technique using image processing for bolt joints in steel bridges[C]//The 2015 World Congress on Advances in Structural Engineering and Mechanics(ASEM15). Korea: Advances in Structural Engineering and Mechanics, 2015, 1-19.
[9] Park J H, Huynh T C, Choi S H, et al.Vision-based technique for bolt-loosening detection in wind turbine tower[J]. Wind Struct, 2015, 21(6): 709-726.
[10] Cha Y J, You K, Choi W. Vision-based detection of loosened bolts using the Hough transform and support vector machines[J]. Automation in Construction, 2016, 71(0): 181-188.
[11] Shull P J, Nguyen T C, Huynh T C, et al. Bolt-loosening identification of bolt connections by vision image-based technique[J]. Proceedings of SPIE - The International Society for Optical Engineering, 2016, 9804(0): 980413.
[12] Liu Y, Huo L S, Song G B. Automatic detection on the bolt loose based on digital image processing[C]// The 2018 Structures Congress(Structures18). Korea: Structures Congress, 2018, 1-22.
[13] Xie Y , Sun J. On-line bolt-loosening detection method of key components of running trains using binocular vision[C]//LIDAR Imaging Detection and Target Recognition 2017. China: Proceedings of SPIE, 2017, 1060513.1-9.
[14] Zhao X, Zhang Y, Wang N. Bolt loosening angle detection technology using deep learning[J]. Structural Control and Health Monitoring, 2018, 26(2014).
[15] Ramana L, Choi W, Cha Y J. Fully automated vision-based loosened bolt detection using the Viola–Jones algorithm[J]. Structural Health Monitoring, 2019, 18(2): 422-434.
[16] Pan X, Yang T Y. Image-based monitoring of bolt loosening through deep-learning-based integrated detection and tracking[J]. Computer-Aided Civil and Infrastructure Engineering, 2022, 37(10): 1207-1222.
[17] Sun Y, Li M, Dong R, et al. Vision-based detection of bolt loosening using YOLOv5[J]. Sensors, 2022, 22(14): 5184(0): 1-16.
[18] Yu Y, Liu Y, Chen J, et al. Detection method for bolted connection looseness at small angles of timber structures based on deep learning[J]. Sensors, 2021, 21(9): 3106(0): 1-19.
[19] Gong H, Deng X, Liu J, et al. Quantitative loosening detection of threaded fasteners using vision-based deep learning and geometric imaging theory[J]. Automation in Construction, 2022, 104009(133): 1-15.
[20] Yang M, Luo L, Tao M. Efficient rail repair machine based on image recognition technology[J]. Journal of Physics: Conference Series, 2020, 1486(4): 042023.1-7.
[21] Yang X, Gao Y, Fang C, et al. Deep learning-based bolt loosening detection for wind turbine towers[J]. Structural control and health monitoring, 2022, 29(6): 1-23.
[22] Wang Q, Li H, Chen Z, et al. Research on double-sided detection method of bolt looseness based on machine vision[J]. Journal of the Brazilian Society of Mechanical

Sciences and Engineering, 2023, (99)45: 1-12.
[23] Deng, X J, Liu J H, Gong H, et al. Detection of loosening angle for mark bolted joints with computer vision and geometric imaging[J]. Automation in Construction, 2022, 142(0), 104517.1-15.
[24] Wang Ruifeng, Wang Ruifeng, Li Hu, et al. Research on the volume detection method of bolts and pre-tightening of rail vehicle bolts [J/OL]. Journal of Railway Science and Engineering: 1-14.
[25] Qi Y, Li P, Xiong B, et al. A two-step computer vision-based framework for bolt loosening detection and its implementation on a smartphone application[J]. Structural Health Monitoring, 2022, 21(5): 2048-2062.
[26] Zheng X, Lei Q, Yao R, et al. Image segmentation based on adaptive K-means algorithm[J]. EURASIP Journal on Image and Video Processing, 2018(1): 1-10.
[27] Otsu N . A Threshold Selection Method from Gray-Level Histograms[J]. IEEE Transactions on Systems Man & Cybernetics, 2007, 9(1): 62-66.
[28] Gonzalez R.C., Woods R.E., Eddins S.L. (2018). Digital Image Processing (4th ed.). Pearson.
[29] MathWorks. atan2 - four-quadrant arctangent [EB/OL], https://ww2.mathworks.cn/help/matlab/ref/atan2.html?s_tid=srchtitle_atan2_1.